Efficient Inspection for Gas Pipes by Infrared Thermography

Hideki ENDO*[1], Takuya KUSAKA*[1]
*[1] Research & Development Dept., SHINKO INSPECTION & SERVICE, CO., LTD.

Gas pipe failure caused by inner corrosion defects is one of the risk factors for the unscheduled shutdown of a plant. The pipes must be inspected to reduce the risk, but this requires a great amount of time and money, since gas pipes are quite long. This research proposes a screening method for the efficient inspection of gas pipes caused by aqueous corrosion. This screening method consists of three stages and includes thermographic and ultrasonic testing. We have developed new thermographic testing to find sludge in a pipe and to measure its wall-thinning distribution. The measuring principle and examples of the application of thermographic testing are introduced in this paper.

Introduction

Plants constructed in the 1960s, during the period of rapid economic growth, have already been operating for several decades. Once aged, main facilities generally have a higher probability of failure in their component equipment, increasing the maintenance cost and the risk of losing production opportunities due to facility shutdown. Thus, at manufacturing (MONODZUKURI) sites, it has become increasingly important to make facility maintenance plans and implement them before failure occurs. It is also important to establish an inspection technology for detecting symptoms of failure at the earliest stage possible.

In a steelworks, the major facilities for iron and steel making are repaired or renewed in a planned manner. Meanwhile, in order to secure the soundness of pipes, the wall thickness of each pipe must be measured by ultrasonic thickness gauges, for example, to ensure that sufficient thickness remains. A steelworks, however, has pipes that may extend for several tens of kilometers in total, and these pipes are usually installed in high places. Thus, inspecting the entire pipe surface to evaluate its soundness requires an enormous amount of time and money.

This paper introduces the results of a study on an efficient inspection method for pipes. The method combines infrared thermography with ultrasonic wave thickness measurement: the former allows remote non-contact testing over the surface of inspection objects (i.e., gas pipes), and the latter has a superior quantitative capability, despite its point measurement nature.

1. Approach to problems of pipe inspection

The pipes that are the subject of this paper are metallic gas pipes, each being of a large caliber, with bases on the ground, and extending for several kilometers. The causes of pipe rupture include aqueous corrosion resulting from sludge that mainly consists of water and accumulates inside the pipe over an extended period of time. Observations on an actually ruptured pipe have revealed a case where the corrosion had progressed particularly in the pipe wall near the position of the interface where the sludge and inner gas fluid came in contact. This implies that it is important to grasp the wall thinning occurring near the interface of the sludge. The above knowledge indicates that measuring the presence/absence of the sludge, its interface position and the distribution of wall thinning in its vicinity can be of great help in determining the priority of repairs.

The conventional diagnosis of pipe deterioration includes visual inspection and/or thickness measurement by ultrasonic wave. There are, however, problems: a visual inspection cannot detect corrosion on the inner surface of a pipe, and thickness measurement by ultrasonic wave can only be performed at representative points and can easily miss inner surface corrosion progressing locally near the interface. Furthermore, in cases where the inner fluid pressure is high, a pipe may rupture where its wall has become thin, which restricts inspection. Thus, conventional inspection techniques alone were unable to achieve efficient screening.

In order to solve these problems, it was decided to proceed with the test in the following three stages:

First stage:

Confirming the presence/absence of sludge in a pipe by an infrared thermographic camera using a passive method (a test method based on infrared radiation from a measured subject without providing the subject with any artificial temperature change). If sludge is detected, the test proceeds to the second stage. If no sludge is detected, the test is "suspended."

Second stage:

Detecting the presence/absence of a part with a high rupture risk, a part in which corrosion has progressed near the sludge interface, and is in the category of "pipe-wall thickness requiring immediate repair," or worse. This detection is conducted using an infrared thermographic camera by an active method (a test method involving heating or cooling of the measured subject to create artificial temperature change). When a thin-walled portion is detected, thickness measurement using ultrasonic wave is omitted due to the risk of rupturing. Otherwise, the test proceeds to the third stage.

Third stage:

If the second stage test detects a thin-walled portion near the sludge interface that falls into the category of "pipe-wall thickness requiring follow-up" or better, the thickness of this part is quantified using an ultrasonic thickness gauge. If no part is detected as being in the category of "pipe-wall thickness requiring follow-up," or better, the test is "suspended."

The criteria for detecting "pipe-wall thickness requiring immediate repair" and "pipe-wall thickness requiring follow-up" are determined in advance using simulation specimens.

The above three-stage test was used for screening the test subject pipes into three categories: i.e., "immediate repair", "follow-up" and "suspended". This concept is based on "triage" in the medical field, a technique for determining the priority of rescue when there are many injured or sick persons.[1), 2)] If appropriate repairs are performed in the order of pipes with higher risk, the risk of plant shutdown is expected to be reduced effectively and significantly. The following describes the method of detecting sludge by an infrared thermographic camera, used to determine the criteria for the categories, and the method for measuring the wall thinning distribution.

2. Method for detecting sludge

In a pipe, sludge and gas exist in separate areas. Thus, when a varying thermal load is applied to the pipe, these areas return different thermal responses. This enables to determine the interface positions of sludge by an infrared thermographic camera by measuring the nonsteady temperature distribution appearing on the outer surface of the pipe. The following describes two possible cases of thermal load variation applied to a pipe:

(a) a case where thermal load applied from inside the pipe varies due to a change in the flow rate and/or temperature of gas flowing through the pipe; and
(b) another case where thermal load applied from outside the pipe varies due to the change in external environment, such as variations in solar radiant energy and air temperature.

Here, the latter case, (b), was chosen, as it frequently offers opportunities for actual measurement; heat transfer analysis and basic experiments using a simulated gas pipe were conducted, and the test conditions were studied.

2.1 Heat transfer analysis based on finite element method (FEM)

To clarify the qualitative trend for the conditions that enable the measurement of sludge inside a pipe, using the temperature distribution on the outer surface of the pipe, a heat transfer analysis was conducted, based on the finite element method (FEM). A varying thermal flux was applied to the outer surface and to the wall of a pipe to qualitatively study its effect.

(1) Analysis model and analysis conditions

Under the conditions that maximize the temperature difference caused by the presence/absence of sludge, the possibility of detecting the interface by thermal imaging was confirmed. In order to accomplish this, the temperature distribution appearing on the pipe surface was estimated by two-dimensional steady-state heat conduction analysis based on FEM. The pipe wall was assumed to approximate a flat plate. The analysis model is shown in **Fig. 1**, while the material constants used are listed in **Table 1**.

Since the sludge has been confirmed to mainly consist of water, the material constants of water were

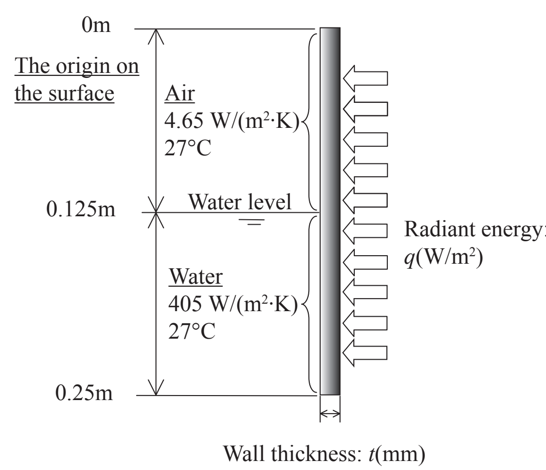

Fig. 1 FEM model

Table 1 Material constants used in the simulation

Mild steel	Density	7860 kg/m^3
	Specific heat	473 J/(kg·K)
	Thermal conductivity	51.6 W/(m·K)

used. This analysis disregards the increase in the temperature of air and water. The analysis also takes into account the heat transfer between the pipe and air and that between the pipe and water; however, it disregards the heat transfer between the air and water. The wall thicknesses were 6mm and 12mm. The thermal fluxes were assumed to be 800W/m^2, the value measured under fine weather in July, and 200W/m^2, under slightly overcast conditions.

(2) Analysis results

First, the effect of thermal flux value was studied. **Fig. 2** shows the temperature distributions on the outer surface of a pipe for the thermal fluxes, incident upon the 6mm thick plate, of 200W/m^2 and 800W/m^2. It is shown that the greater the thermal flux value, the greater the temperature difference between the air and water, making it easier to detect the sludge.

Next, the effect of pipe-wall thickness was studied. **Fig. 3** shows the temperature distributions on the outer surface of a pipe for the thermal flux of 800W/m^2 and pipe-wall thicknesses of 6mm and 12mm. It can be seen that the thinner the plate, the greater the temperature difference between the air and water becomes, making detection easier. For each condition analyzed this time, however, a temperature gradient was found at the position of the interface. It was found that this makes it difficult to determine the interface position of the sludge from the surface temperature distribution.

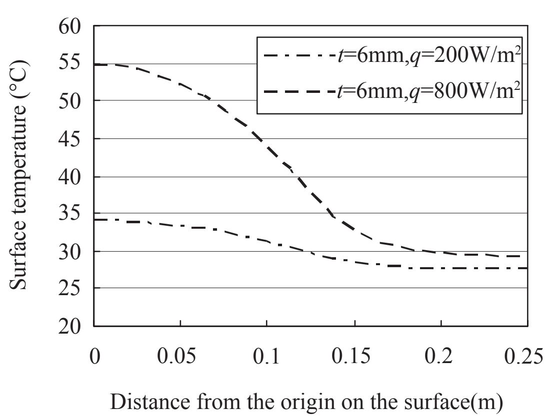

Fig. 2 Relation between radiant energy and temperature difference on the surface

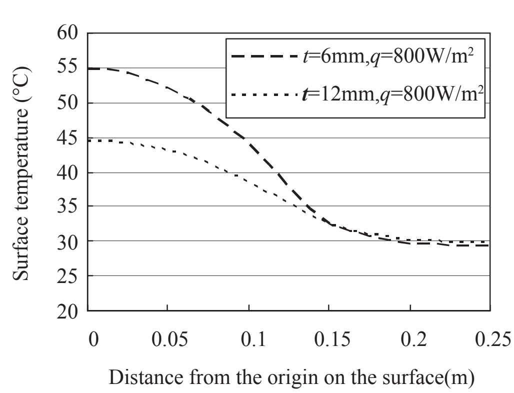

Fig. 3 Relation between wall thickness and temperature difference on the surface

2.2 Estimation of interface position using differential progression

In the past, the level of sludge accumulated on the bottom of a petroleum tank or the like was determined by estimating the interface position of the sludge from thermal images taken at certain moments.[3] This method, however, relies thoroughly on workers in determining the interface on thermal images. Thus, when no clear boundary is found, the detected interface position may vary depending on the workers. However, in view of this, a convenient method for detecting the interface has been devised in which the first differential progression is calculated for the temperature values along a line drawn on a thermal image so that estimation can be made from the local minimum or maximum point.

(1) Study based on numerical simulation

The surface temperature distribution obtained in Section 2.1, (2) was used to calculate the first differential progression to determine the interface position, and the results are shown in **Fig. 4**. For all the conditions, the interface position agrees with the position of local minimum point. The differential progression processing has a feature similar to differential processing and yields a minimum or maximum value at the interface where the temperature variation is greatest in the surface temperature distribution. It was found to be possible to detect the interface by obtaining the temperature distribution along a line crossing the interface in the thermal image and by calculating the first differential progression.

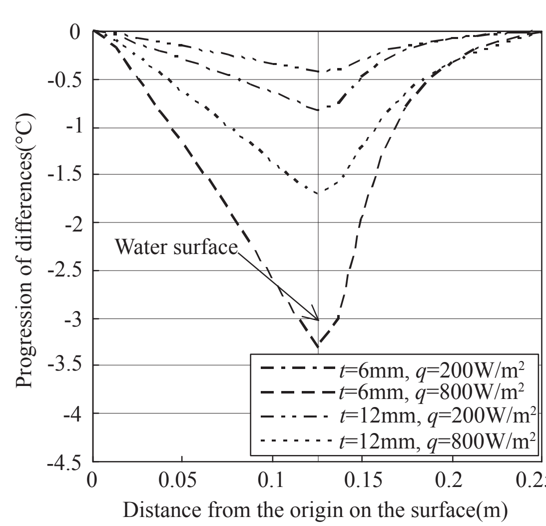

Fig. 4 Relation between local minimum point and water surface

(2) Test using simulated gas pipe

A simulated gas pipe (diameter, 300mm; length, 1,000mm; thickness, 3.2mm) was placed horizontally with water poured into it to a depth of 60mm to simulate sludge. Thermal images were taken every hour from 10 am to 3 pm, from below the pipe at an obliquely upward angle of 45 degrees. **Fig. 5** shows a typical example of the measurement. Fig. 5 (b) is the thermal image, and Fig. 5 (c) shows the temperature distribution along the data processing line (shown by a dotted line) in Fig. 5 (b). The differential progression was calculated from Fig. 5 (c), the results being shown in Fig. 5 (d). Fig. 5 (d) demonstrates a good agreement between the local minimum point and the interface of the water. However, since pipe surfaces are curved, the pipe end portion in the image is susceptible to the disturbance of reflection due to the angle dependence of emissivity, which caused another local minimum point to appear also to the left of the true interface. Therefore, when determining the interface, several thermal images must be taken, not only from the oblique angle of 45 degrees, but also from various other angles, for a comprehensive judgment to be made.

(3) Evaluation by testing real pipes

Fig. 6 shows an example of measurement conducted on a gas pipe actually in use. It was confirmed by a radiographic test that sludge existed in a portion extending from the bottom to a position at 250mm of the ϕ1,200mm pipe. As in the case of the simulated gas pipe, the first differential progression was calculated for the central portion, A, of the area heated by the sun. Then a local minimum point appeared at a position approximately 230mm from the bottom. This agreed closely with the result of the radiographic test. The thermal image showed

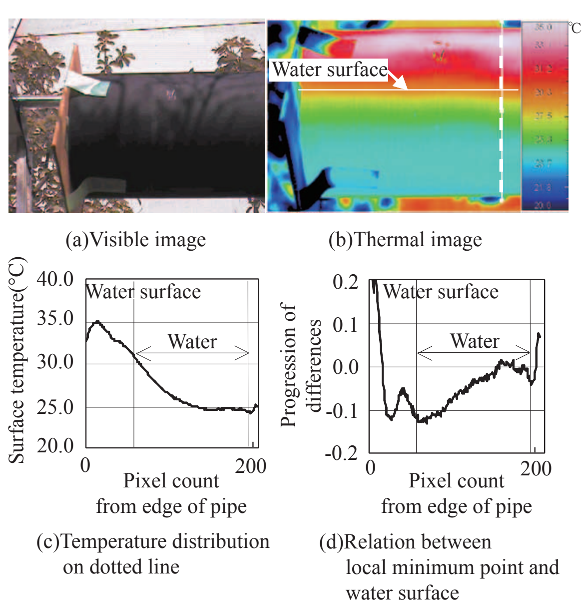

Fig. 5 Example of measurement of simulated gas pipe

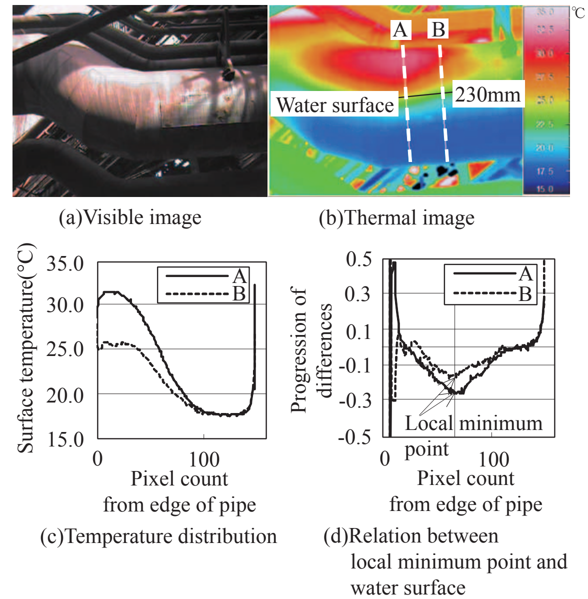

Fig. 6 Example of gas pipe measurement

the interface as if it were oblique. Thus, a new data processing line B was provided to the right of line A for comparison. As shown in Fig. 6 (d), both lines A and B indicated almost the same interface position. This result confirms the validity of the estimation method based on the first differential progression.

3. Method for measuring wall thinning distribution

The recent improvement in the temperature resolution of infrared thermographic cameras has facilitated the estimation of inner defects from several images of nonsteady temperature distribution captured at specific moments. This estimation of defects, however, is made from specific thermal images and is influenced by, for example, reflections from the surroundings, which often makes it difficult to estimate the defects. Against this backdrop, various methods have been studied to estimate defects by the signal processing of thermal images measured chronologically.[4)] Now, a convenient method has been devised for obtaining the wall thinning distribution while reducing the influence of disturbance. The method calculates the correlation coefficient of temperature change among the pixels of thermal images chronologically measured and thereby detects parts with significantly reduced thickness as the distribution of the correlation coefficients.

3.1 Study on validity of measuring wall-thinning distribution based on correlation coefficients

Using a specimen with flat-bottomed hole defects simulating locally thinned areas, a study was conducted on the issues of measuring wall-thinning distribution. Measures against these issues were also studied. **Fig. 7** shows the details of the specimen used for this study. A 2.3kW halogen heater was placed at a position approximately 0.2m away from the specimen, which then was step-heated for approximately 20 seconds. Thermal images during and after the heating were continuously recorded at a frame rate of 5 frames per second by an infrared thermographic camera. **Fig. 8** shows a thermal image taken 3 seconds after the start of heating. The flat-bottomed hole defect in the middle of the specimen exhibits an area with a temperature higher than the surrounding area, allowing the detection of the wall thinning. Above this area, however, a zone affected by reflection caused by the halogen heater was observed, and this zone caused a higher apparent temperature to be measured. This is due to the fact that the reflected object, or halogen heater, has a much higher temperature than the specimen temperature, making the reflection from the specimen not negligible. The following signal processing was performed to distinguish defects from this disturbance.

The changes in temperature were measured chronologically at points "a" to "e" in the thermal image shown in Fig. 8, and the results are shown in **Fig. 9**. At a defect-free point, the temperature rises stepwise at the beginning of the heating and then increases linearly with a constant slope. Meanwhile, at a point with a flat-bottomed hole defect, the temperature tends to change gradually at

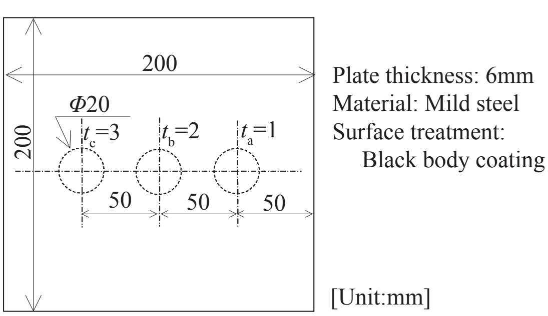

Fig. 7 Dimension of specimen with flat-bottomed hole defects

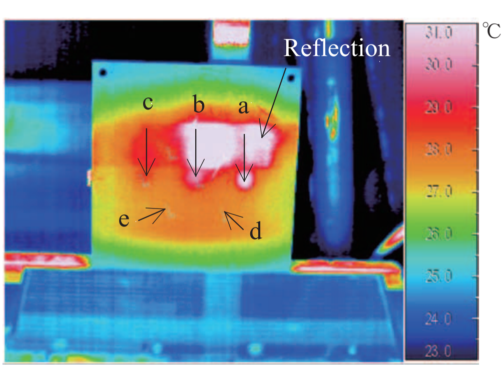

Fig. 8 Thermal image at 3 sec after starting step heating

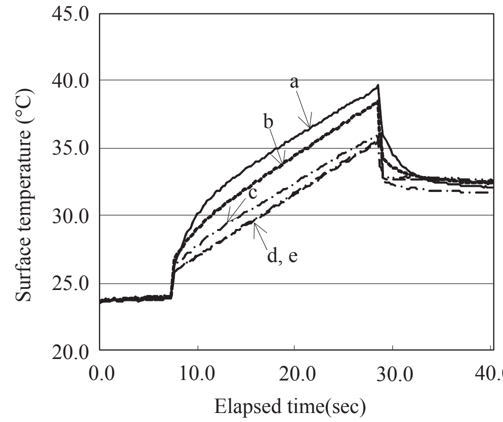

Fig. 9 Relation between surface temperature and elapsed time

the beginning of the heating and then converge into a certain slope at the end. In addition, the thinner the remaining thickness under the flat-bottomed hole defect, the longer it takes before the convergence results in a certain slope. To digitize this difference in tendency, a defect-free point was selected to determine the correlation coefficient r with other pixels of chronological temperature change during the heating process. The correlation coefficient r was calculated by Equation (1):

$$r=\frac{\sum_{i=1}^{n}(x_i-\bar{x})(y_i-\bar{y})}{\sqrt{\sum_{i=1}^{n}(x_i-\bar{x})^2}\sqrt{\sum_{i=1}^{n}(y_i-\bar{y})^2} \quad \cdots\cdots\cdots\cdots\cdots\cdots (1)$$

wherein x_i represents the chronological temperature change of the defect-free point, and y_i represents the chronological temperature change of each pixel. Further, $\bar{x}$ and $\bar{y}$ represent the average values of x_i and y_i, respectively. The correlation coefficient r means normalizing x_i and y_i so as to make their averages zero and variances 1, to determine the covariance. The influence of reflection is removed by normalizing the temperature change.

Thermal images were taken during 20 seconds of step heating. In the thermal images, the chronological temperature change at point "e" is regarded as that of the defect-free point. From this, a correlation coefficient distribution of each pixel was determined and the result is shown in **Fig.10**. The signal processing ignored the time zones right before the beginning and after the cessation of heating, during which the temperature changed stepwise at the defect-free point, but instead used the gradual temperature change during the step heating. In Fig.10, the three defects with flat bottoms are observed in the middle of the specimen, showing that the thinner the remaining thickness, the smaller the correlation coefficient becomes. Comparing Fig. 8 and Fig.10, the image for correlation coefficient distribution shows a significantly reduced

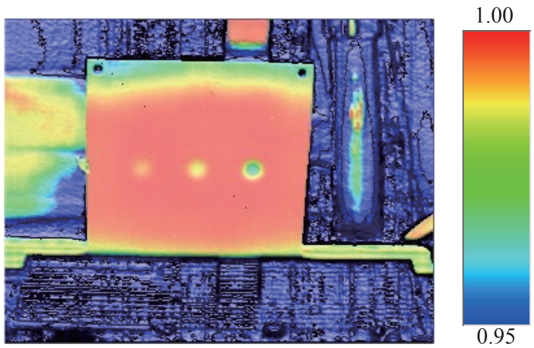

Fig.10 Correlation coefficient distribution on thermal image

disturbance due to reflection, providing clear views of the defects.

3.2 Application to actual pipes

Fig.11 shows an evaluation example of the wall-thinning distribution of a pipe used in an actual plant. The measured part included wall thinning that had been repaired from the outside. There, however, was a possibility of the repaired area not covering the entire area with a thinned wall. Thus the present technique was used for the evaluation. When taking thermal images, no processing was done on the measurement surface to convert it to a quasi-blackbody, since adhered dust and the like can lead to the same effect as the quasi-blackbody processing. Fig.11 (b) is a thermal image taken by an infrared thermographic camera set up almost directly facing the repaired area. Here, the repaired area exhibits an apparent surface temperature that measured significantly higher than its periphery. This results in a low contrast in the periphery of the repaired area. Also, since a halogen heater was used, uneven thermal flux in the irradiated area resulted in uneven heating. The thermal image includes the influence of these factors as disturbance. Therefore, in Fig.11 (b) alone, it was difficult to detect the minute change of surface temperature caused by wall thinning. Fig.11 (c) shows an image after processing the correlation coefficient, in which a defect-free point indicated by an arrow in Fig.11 (b) was selected from the pixels exhibiting temperature changes greater than 5℃ caused by the heating. The processing of the correlation coefficient normalizes the chronological temperature change, reducing the effect of uneven heating caused by the halogen heater. As a result, the area suspected to have undergone wall thinning is clearly shown in the periphery of the repaired area. The wall thickness was measured on a later day by an ultrasonic thickness gauge, which confirmed how wall thinning occurred smoothly towards the repaired area. At that time, the wall thickness at point "a" was approximately 13% of the defect-free point, while the wall thickness at point "b", neighboring point "a", was approximately 45% of the defect-free point. This result confirms that determining the correlation coefficient distribution allows the detection of the part with significant wall thinning. The future plan includes a study on the effect of sludge inside a pipe, the pipe surface and the like, on the surface temperature, so as to expand the applicability of this detection method.

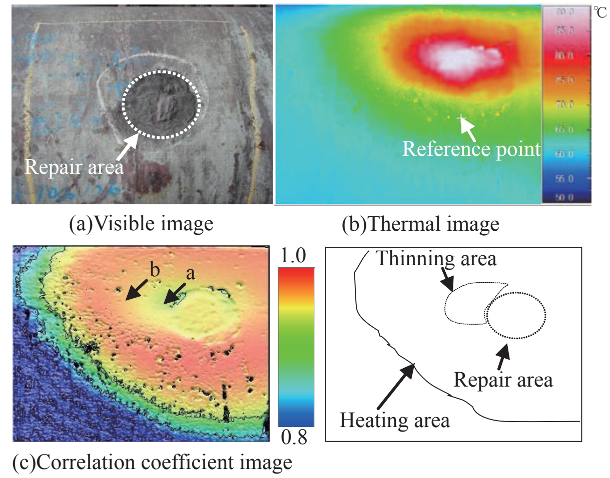

Fig.11 Example of pipe measurement

Conclusions

A screening method was proposed in order to efficiently confirm the soundness of gas pipes used in steelmaking plants. This method is based on triage techniques employed in the medical field and uses the test results obtained by an infrared thermographic camera and ultrasonic thickness gauge as determination criteria. Aiming at evaluating the wall thinning caused by aqueous corrosion due to sludge in pipes, an infrared thermographic camera was used to conduct studies to find a method for detecting sludge inside a pipe and a method for measuring the distribution of wall thinning. Testing conditions, signal processing, etc., were developed and adapted for actual pipes, and their validity was confirmed.

References

1) T. Sakagami. *Petrotech*. 2009, Vol.32, No.3, p.153.
2) Saga EMS conference, Disaster task force, Disaster medical manual workgroup, *Disaster Medical Response Manual, Saga prefecture*. 2003, pp.29-42.
3) T. Sakagami et al. *Proceedings of the 15th JSME design and systems division conference*. 2005, pp.480-481.
4) JSNDI Ad Hoc Research and Technical Committee on Thermography. *Handbook of nondestructive testing*. 2004, pp.169-175.